IEEE Access
Multidisciplinary | Rapid Review | Open Access Journal

Received May 5, 2020, accepted June 7, 2020, date of publication June 22, 2020, date of current version July 2, 2020.

Digital Object Identifier 10.1109/ACCESS.2020.3004074

Coherent Integration Algorithm for a Maneuvering Target Based on Frequency Spectrum Segment Processing

JINZHI XIANG[1,2], WEI CUI[1], (Member, IEEE), AND JING TIAN[1], (Member, IEEE)
[1]School of Information and Electronics, Beijing Institute of Technology, Beijing 100811, China
[2]Beijing Institute of Radion Measurement, Beijing 100854, China

Corresponding author: Wei Cui (cuiwei@bit.edu.cn)

This work was supported by the National Natural Science Foundation of China under Grant 61701030.

ABSTRACT This paper considers the coherent integration problem for a low-observable maneuvering target, where the velocity and acceleration result in range migration (RM) and Doppler frequency migration (DFM) within the coherent pulse interval. A novel method based on the frequency spectrum segment processing (FSSP) and the segmental Lv's distribution (SLVD) is proposed to realize the long-time coherent integration for multiple maneuvering targets. In this method, FSSP is proposed to eliminate the RM effect by dividing the received signal into several subband signals and expanding the range resolution of the subband signals. Then SLVD is applied to achieve the coherent integration of the subband signals and accumulate the energy of all the subband signals coherently. The proposed method can realize the coherent integration for multiple maneuvering targets without any prior knowledge of the targets' motion. The simulation and experimental results demonstrate the effectiveness of the proposed algorithm.

INDEX TERMS Maneuvering target detection, long-time coherent integration, frequency spectrum segment processing (FSSP), segmental Lv's distribution (SLVD).

I. INTRODUCTION

With the development of stealth technique and highly maneuvering target, such as stealth craft, unmanned aerial vehicle, and ballistic missile etc, the long-time integration and detection of the low-observable maneuvering targets attract growing attentions in modern radar [1]–[5]. In general, the radar echoes of the weak and maneuvering targets have several characteristics: 1) Low signal-to-noise ratio (SNR); 2) High-speed or high maneuverability [5]. It is well-known that the long-time coherent integration is an effective way to increase the SNR of radar echoes and improve the detection performance by compensating the phase fluctuation among different pulses [6]. The coherent integration can almost achieve linear integration gain with the number of pulses [5], [6]. Therefore, long-time coherent integration is an effective way to detect low-observable maneuvering targets.

However, the motion of maneuvering target may result in range migration (RM) and Doppler frequency migration (DFM) within the long coherent pulse interval, which will result in serious performance loss in the long-time coherent integration for a maneuvering target [24]. To realize good coherent integration performance and further improve the detection performance, RM and DFM should be corrected for the coherent integration processing. In [8], a popular method named keystone transform was proposed to correct the RM without a priori motion information of the target, which correct the RM by rescaling the slow time axis for each range frequency. It is widely employed to correct the RM in synthetic aperture radar (SAR) imaging and long-time coherent integration [8]–[14]. Recently, a method based on keystone transform and time reversing transform (KT-TRT) was proposed for SAR imaging of ground moving targets, which is computationally efficient at the cost of serious performance loss in low SNR scenarios [15].

To eliminate the DFM effect on coherent integration, several typical methods have been proposed, such as the phase matching approach [16], dechirp method [17], chirp-Fourier transform [18], and fractional Fourier transform (FRFT) based methods [19], etc. Recently, a type of time-frequency transform methods named as Lv's distribution (LVD), has been proposed in [20], which realizes the coherent integration and estimates the parameters of the chirp signals without using any searching operation. The LVD breaks through the tradeoff between the resolution and the cross terms [20], [21]. In [22], a method named subband dual-frequency

The associate editor coordinating the review of this manuscript and approving it for publication was Hasan S. Mir.

conjugate-Lv's transform (SDFC-LVD) was proposed to correct RM and DFM, which can resolve the Doppler ambiguity problem when keystone transform is applied and has a low computational complexity. However, it degrades the parameter estimation accuracy.

In [7], a maximum likelihood estimation method named the generalized Radon-Fourier transform (GRFT) was proposed to correct RM and DFM during the integration time simultaneously and estimate the parameters of maneuvering targets with arbitrary order motion. However, it requires jointly multidimensional searching and is computationally prohibitive. Based on the Radon transform and different time-frequency techniques, the Radon-Lv's distribution (RLVD) [23], the Radon-fractional Fourier transform (RFRFT) [24], and the Radon-linear canonical ambiguity function (RLCAF) [25] were proposed to realize the long-time coherent integration, which can not only eliminate the RM effect via jointly searching the trajectory of the target in the motion parameters space, but also remove the DFM via the time-frequency analysis methods. However, these methods are often computationally prohibitive.

To deal with the problems of RM and DFM, this paper proposes a method based on the frequency spectrum segment processing (FSSP) and the segmental Lv's distribution (SLVD) to realize the long-time coherent integration for multiple maneuvering targets. In this method, the frequency spectrum segment processing (FSSP) is firstly proposed to divide the radar echoes into several subband signals and expand the range cell of all the subband signals, which eliminates the RM effect on coherent integration of the subband signals. Then the segmental Lv's distribution (SLVD) is performed to realize the coherent integration of each subband signal along the slow time axis and accumulate the energy of all the subband signals coherently. Numerical experiments using both simulated and real data are provided to verify the effectiveness of the proposed method.

The rest of this paper is organized as follows. In Section II, the signal model is presented. In Section III, a method based on FSSP and SLVD is proposed to achieve the long-time coherent integration for multiple maneuvering targets. In Section IV, the computational complexity of the proposed method is analyzed. In Section V, the numerical experiments are performed. Finally, in Section VI, some conclusions are given.

II. SIGNAL MODEL

Suppose that the radar transmits a normalized linear frequency modulated (LFM) signal, i.e.,

$$s_t(t_n,\tau)=\mathrm{rect}\left(\frac{\tau}{T_p}\right)\exp(j\pi\gamma\tau^2)\exp\left[j2\pi f_c(t_n+\tau)\right], \quad (1)$$

where

$$\mathrm{rect}(x)=\begin{cases}1, & |x|\le\frac{1}{2}\\ 0, & |x|>\frac{1}{2}\end{cases} \quad (2)$$

T_p is the pulse duration, $\gamma=B/T_p$ is the chirp rate of LFM signal with bandwidth B, f_c is the carrier frequency, τ is the fast time, $t_n=nT_r$ $(n=0,1,\ldots,N-1)$ is the slow time, N denotes the number of the coherent integrated pulses, T_r is the pulse repetition time.

Suppose that there are K maneuvering targets in the scene and the targets are point-scattering objects. Neglecting the high-order components, the instantaneous slant range $r_k(t_n)$ of the kth maneuvering target with a constant acceleration satisfies

$$R_k(t_n)=r_k+v_kt_n+0.5a_kt_n^2, \quad (3)$$

where r_k, v_k, and a_k denote the initial range, the radial velocity, and the radial acceleration between the kth target and the radar, respectively.

According to [27], the varying phase and amplitude of the received signal caused by the fluctuated backscattering have an effect on the coherent integration. In this paper, the Swerling 0 model is considered and the backscattering coefficient (or the radar cross section (RCS)) of the target is assumed to be fixed [28].

The echoes of the K targets after down conversion can be expressed as

$$\begin{aligned}s_r(t_n,\tau)=&\sum_{k=1}^{K}A_k\mathrm{rect}\left(\frac{\tau-\tau_k}{T_p}\right)\exp\left[j\pi\gamma\left(\tau-\tau_k\right)^2\right]\\&\times\exp\left(-j2\pi f_c\tau_k\right),\end{aligned} \quad (4)$$

where A_k is the backscattering coefficient of the kth target, $\tau_k=2R_k(t_n)/c$, c is the light speed.

Construct the matched filter

$$h(\tau)=\mathrm{rect}\left(\tau/T_p\right)\exp(-j\pi\gamma\tau^2). \quad (5)$$

Then the received signal after pulse compression in range-frequency domain can be expressed as

$$\begin{aligned}S_p(t_n,f)=&\underset{\tau}{\mathrm{FT}}\left[s_r(t_n,\tau)\right]\underset{\tau}{\mathrm{FT}}\left[h(\tau)\right]\\=&\sum_{k=1}^{K}A_k\mathrm{rect}\left(\frac{f-f_k/2}{B+f_k}\right)\exp\left(j\frac{2\pi f_kf}{\gamma}\right)\\&\times\exp\left[-j\frac{4\pi(f_c+f-f_k)R_k(t_n)}{c}\right],\end{aligned} \quad (6)$$

where $\mathrm{FT}_\tau(\cdot)$ denotes the Fourier transform over τ, f is the range frequency corresponding to τ.

By applying inverse Fourier transform on (6), the received signal of the targets after pulse compression can be expressed as

$$\begin{aligned}s_p(t_n,\tau)=&\underset{f}{\mathrm{IFT}}\left[S_p(t_n,f)\right]\\=&\sum_{k=1}^{K}A_kG_1\mathrm{sinc}\left[B'(\tau-\frac{2R_k(t_n)}{c}+\frac{f_k}{\gamma})\right]\\&\times\exp\left[-j2\pi(f_c-f_k)\frac{2R_k(t_n)}{c}\right],\end{aligned} \quad (7)$$

where $\mathrm{IFT}_f(\cdot)$ denotes the inverse Fourier transform over f, $\mathrm{sinc}(x)$ denotes the sinc function, $B' = B - |f_k|$, G_1 is the pulse compression gain of the signal, and satisfy $G_1 = BT_p$.

It can be seen from (7) that the envelope and the Doppler frequency of the targets are time variant and RM and DFM would occur during the long integration interval, which will make it difficult to integrated the energy of the targets effectively [10], [11].

III. COHERENT INTEGRATION METHOD

In this section, a method based on FSSP and SLVD is proposed to realize the coherent integration for multiple maneuvering targets.

A. RM CORRECTION VIA FSSP

As we know, if the envelope offset of the received signal does not exceed the range resolution, the RM effect on the coherent integration can be ignored. Based on this consideration, the FSSP is proposed to expand the range cell by dividing the range frequency spectrum of each echo into M segments. The M subband signals are constructed.

Since f_k/γ is almost fixed and $f_k \ll f_c$, ignore the effect of f_k on the coherent integration. The mth subband signal can be written as

$$S_s(t_n, f, m) = \sum_{k=1}^{K} A_k \mathrm{rect}\left(\frac{f - f_s(m)}{B_s}\right) \times \exp\left[-j2\pi(f_c + f)\frac{2R_k(t_n)}{c}\right], \quad (8)$$

where $B_s = B/M$ is the bandwidth of each subband signal, m is the number of subband signals which satisfies $m = [1, 2, \ldots, M]$, and $f_s(m) = -0.5B + (m - 0.5)B_s$.

Then applying IFT on (8) with respect to f, we have

$$s_s(t_n, \tau, m) = \sum_{k=1}^{K} A_k G_2 \mathrm{sinc}\left[B_s\left(\tau - \frac{2R_k(t_n)}{c}\right)\right] \times \exp\left(-j2\pi f_s(m)\tau\right) \times \exp\left[-j2\pi(f_c + f_s(m))\frac{2R_k(t_n)}{c}\right], \quad (9)$$

where G_2 is the pulse compression gain of each subband signal and $G_2 = B_s T_p$.

Clearly, the range resolution of each subband signal can be expressed as

$$\rho_{r2} = \frac{c}{2B_s} = M\rho_{r1}. \quad (10)$$

It can be seen the range resolution of each subband signal is expanded M times. In order to eliminate the effect of RM, the maximum range offset caused by the targets' motion parameters within the coherent integration time should not exceed the range resolution of the subband signal, that is $\max\left(|v_k T_c + 0.5 a_k T_c^2|\right) \le \rho_{r2}$, where $T_c = NT_r$ is the coherent integration time. Therefore, B_s should satisfy

$$B_s \le \frac{c}{|2v_l T_c + a_l T_c^2|}, \quad (11)$$

where $v_l = \max(|v_k|)$ and $a_l = \max(|a_k|)$.

Therefore, we can get

$$M \ge \mathrm{ceil}\left(\frac{B}{B_s}\right). \quad (12)$$

B. COHERENT INTEGRATION VIA SLVD

When the total number M of the subband signals satisfies the condition of (12), the energy of the target is concentrated in the same range cell and the RM effect on the coherent integration of the subband signal has been eliminated. From (9), we can see that the subband signal in the right range cell corresponding to the target can be modeled as a chirp signal in the slow time dimension after FSSP.

According to [20], LVD has excellent parameters estimation performance of chirp signals by integrating the signal energy coherently in the centroid frequency and chirp rate domain. Moreover, LVD can suppress the cross terms effectively and it has the asymptotic linearity. Based on the work of LVD, SLVD is proposed to realize the coherent integration of all the subband signals. The detailed derivation is introduced in the following.

For simplicity, the signal model of the kth target is derived. The mth subband signal corresponding to the range cell of the kth target can be modeled as a chirp signal in the slow time dimension, i.e., $\tau = 2R_k(t_n)/c$, which can be expressed as

$$s_c(t_n, m) = A_k G_2 \exp\left(-j2\pi f_s(m)\tau_k\right) \times \exp\left[-j\frac{4\pi(f_c + f_s(m))R_k(t_n)}{c}\right], \quad (13)$$

The parametric symmetric instantaneous autocorrelation function (PSIAF) of (13) is defined by [20]

$$\begin{aligned} R_c(t_n, t_a, m) &= s_c\left(t_n + \frac{t_a + q}{2}, m\right) s_c^*\left(t_n - \frac{t_a + q}{2}, m\right) \\ &= (A_k G_2)^2 \exp\left[-j\frac{4\pi(f_c + f_s(m))a_k(t_a + q)t_n}{c}\right] \\ &\quad \times \exp\left[-j\frac{4\pi(f_c + f_s(m))v_k(t_a + q)}{c}\right], \end{aligned} \quad (14)$$

where $*$ denotes the complex conjugation operation, t_a is a lag variable and q denotes a constant time-delay.

Unlike the PSIAF of LVD [15, Eq. (2)], the time variable t_n, lag variable t_a and the number of subband signal m coupled with each other in the exponential terms of (14). To remove the coupling of the first exponential term, the scaling operation is performed on t_n for each t_a and m. The scaling transform is defined as follows

$$t_n = \frac{t_l f_c}{h(t_a + q)(f_c + f_s(m))}, \quad (15)$$

where h is a scaling factor. For easy implementation, we can choose the parameters $h = 1$ and $q = 1$ [20].

Substituting (15) into (14) yields

$$\begin{aligned} R_s(t_l, t_a, m) &= (A_k G_2)^2 \exp\left[-j\frac{4\pi f_c a_k t_l}{c}\right] \\ &\quad \times \exp\left[-j\frac{4\pi(f_c + f_s(m))v_k(t_a + q)}{c}\right]. \end{aligned} \quad (16)$$

By applying FT on (16) with respect to t_l, we can obtain

$$F_a(f_a, t_a, m) = (A_k G_2)^2 N \text{sinc}\left(f_a + \frac{2f_c a_k}{c}\right) \times \exp\left[-j\frac{4\pi(f_c + f_s(m))v_k(t_a + q)}{c}\right]. \quad (17)$$

It can be observed that the coupling between t_a and m still exists in the exponential term in (17), which will affect the parameter estimation. To eliminate the coupling between m and t_a of the exponential term in (17), the phase compensation function related to the velocity is constructed as follows

$$H_v(t_a, m, n_s) = \exp\left[j\frac{4\pi(f_c + f_s(m))n_s v_s(t_a + q)}{c}\right], \quad (18)$$

where n_s and v_s denote the searching number and the searching interval of the velocity, respectively. And $n_s = [-\text{round}(v_l/v_s), -\text{round}(v_l/v_s) + 1, \cdots, \text{round}(v_l/v_s)]$.

Multiplying (18) by (17) yields

$$F_c(f_a, t_a, m, n_s) = (A_k G_2)^2 N \text{sinc}\left(f_a + \frac{2f_c a_k}{c}\right) \times \exp\left[-j\frac{4\pi(f_c + f_s(m))\Delta v_k(t_a + q)}{c}\right], \quad (19)$$

where $\Delta v_k = v_k - n_s v_s$.

Then applying Fourier transform on (19) with respect to t_a, we can obtain

$$L_s(f_a, f_d, m, n_s) = (A_k G_2 N)^2 \text{sinc}(f_a + \frac{2f_c a_k}{c}) \times \text{sinc}\left[f_d + \frac{2(f_c + f_s(m))\Delta v_k}{c}\right] \times \exp\left[-j\frac{4\pi(f_c + f_s(m))\Delta v_k q}{c}\right]. \quad (20)$$

In order to achieve the coherent integration of different subband signals, the offset of the centroid frequency f_d caused by the number of the subband signal m among the different subband signals should be less than half of the frequency resolution, that is $\max[|2(f_s(1) - f_s(M))\Delta v_k/c|] \leq 1/(2T_c)$. So we can derive that $|2B\Delta v_k/c| \leq 1/(2T_c)$. Moreover, the phase variation caused by the number of subband signals m should be less than π, which means the residual velocity should satisfy $|4\pi B\Delta v_k q/c| \leq \pi$. As we know, $|\Delta v_k| \leq 0.5\, v_s$ when $n_s = \text{round}(v_k/v_s)$. Therefore, the combined limit on v_s is

$$v_s \leq \min\left(\frac{c}{2Bq}, \frac{c}{2BT_c}\right). \quad (21)$$

When $n_s = \text{round}(v_k/v_s)$ and v_s satisfies the condition of (21), the LVD result of each subband signal can be obtained and the peak's location of each subband signal is in the same cell in the CFCR domain. Then we can obtain the integrated SLVD result among all the subband signals

$$L(f_a, f_d, n_s) = \sum_{m=1}^{M} L_s(f_a, f_d, m, n_s) = (A_k G_2 N)^2 M \exp\left(-j\frac{4\pi f_c \Delta v_k q}{c}\right) \times \text{sinc}(f_a + \frac{2f_c a_k}{c})\text{sinc}\left(f_d + \frac{2f_c \Delta v_k}{c}\right). \quad (22)$$

It can be seen from (22) that the target's energy is well integrated as a peak. Thus, the maneuvering target detection can be accomplished and the estimates of the motion parameters can be obtained based on the location of the peak. Fig. 1 shows the flowchart of the proposed algorithm.

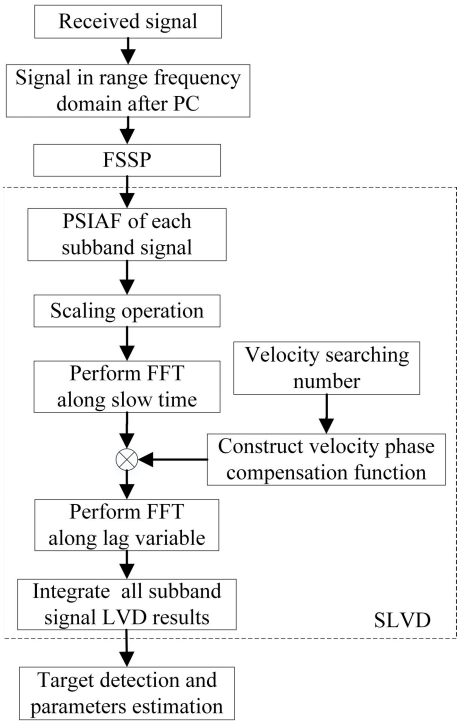

FIGURE 1. Flowchart of the proposed method.

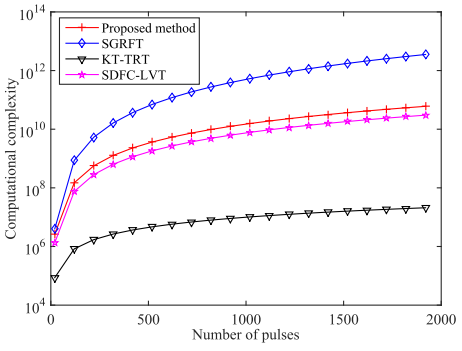

FIGURE 2. Computational complexity versus the number of the integrated pulses.

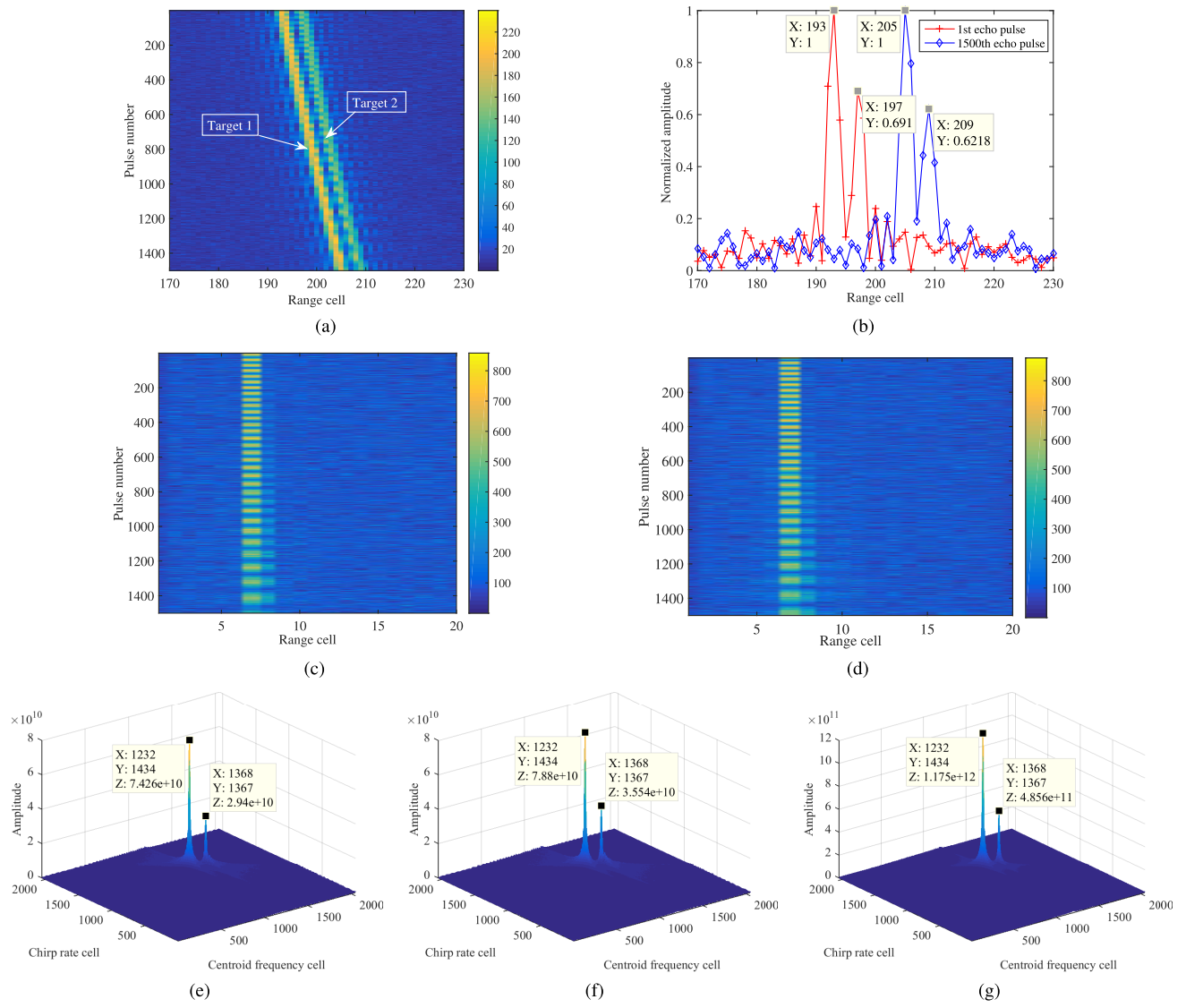

FIGURE 3. Simulation results of the proposed method. (a) Result after pulse compression; (b) Echoes of 1st and 1500th pulses; (c) Result of the first subband signal after FSSP; (d) Result of the last subband signal after FSSP; (e) LVD result of the first subband signal; (f) LVD result of the last subband signal; (g) The integrated LVD result of all the subband signals.

C. OUTPUT SNR ANALYSIS

The detection performance can be examined in terms of the output SNR. According to [29], the output SNR of the proposed method can be defined as

$$\mathrm{SNR}_{\mathrm{SLVD}} = \frac{\left|L_s(\hat{f}_a, \hat{f}_d)\right|^2}{\mathrm{var}\left\{L_{s+v}(\hat{f}_a, \hat{f}_d)\right\}}. \tag{23}$$

where $L_s(\hat{f}_a, \hat{f}_d)$ denotes the SLVD output of the signal only and $L_{s+v}(\hat{f}_a, \hat{f}_d)$ denotes the SLVD output of the signal plus noise.

According to [5], the output SNR of each suband signal after LVD is lower bounded by

$$\mathrm{SNR}_{\mathrm{seg}} \geq \frac{N^2 G_2^2 \mathrm{SNR}_k^2}{2NG_2\mathrm{SNR}_k + 1}. \tag{24}$$

where SNR_k is the input SNR of the original received signal of the kth target before pulse compression.

Therefore, the output SNR of the accumulated result among all subband signals after SLVD is lower bounded by

$$\begin{aligned}\mathrm{SNR}_{\mathrm{SLVD}} &= \mathrm{SNR}_{\mathrm{seg}} M \\ &\geq \frac{N^2 G_1^2 \mathrm{SNR}_k^2}{2NG_1\mathrm{SNR}_k + M}.\end{aligned} \tag{25}$$

It can be observed from (25) that the output SNR of the proposed method can be improved by increasing the total number of the integrated pulses or reducing the total number of the suband signals in low input SNR scenarios.

IV. COMPUTATIONAL COMPLEXITY ANALYSIS

In what follows, the computational complexity of the proposed method will be analyzed. Then the comparisons of the

computational complexity are performed among the proposed method, SDFC-LVT, KT-TRT, and SGRFT.

Let N_r and N be the number of the range cells and the integrated pulses, respectively. As we know, the pulse compression is usually performed in the range frequency domain. For FSSP, $NN_r \log_2(N_r/N_s)$ complex multiplications (CMs) are needed after multiplying by the matched filter, where N_s denotes the number of the subband signals. Compared with the pulse compression performed in the range frequency domain, FSSP does not increase the computational complexity. Let N_{v1} be the searching number of the velocity. According to [20], the computational complexity of the LVD based on the scaled Fourier transform is $3N^2 \log_2 N$. For SLVD, $3N_{v1}N_rN^2 \log_2 N$ CMs are needed. Thus, the computational cost of the proposed method is $O\left[3N_{v1}N_rN^2 \log_2 N\right]$.

According to [22], the computational complexity of SDFC-LVT is $O\left[1.5N_rN^2 \log_2 N + N_rN \log_2 N\right]$. On the other hand, let N_{v2} be the searching number of the velocity ambiguity factor for KT-TRT. According to [15], the computational complexity of KT-TRT is about $O\left[2N_rN_{v2}N^2\right]$. For SGRFT, let N_{v3} and N_{a3} denote the searching numbers of the velocity and the acceleration, respectively. According to [7], the computational complexity of SGRFT is $O\left[N_rN_{v3}N_{a3}N\right]$. For SGRFT, the searching intervals of the velocity and the acceleration should satisfy $v_s \leq \lambda/2T_c$ and $a_s \leq \lambda/2T_c^2$, respectively. According to [15], the searching velocity of KT-TRT is $\lambda/2T_r$. On the other hand, the searching intervals of the velocity of the proposed method satisfies (21). So we can derive approximately that $N_{v3} = NN_{v2}$ and $N_{v3} = QN_{v1}$, where $Q = \min(f_c/(Bq), f_c/(BT_c))$. The computational complexities of the four methods are listed in Table 1.

TABLE 1. Computational complexities of the four methods.

Methods	Computational complexity
Proposed method	$O\left[3N_{v1}N_rN^2 \log_2 N\right]$
SDFC-LVT	$O\left[1.5N_rN^2 \log_2 N + N_rN \log_2 N\right]$
KT-TRT	$O\left[2N_rN_{v2}N^2\right]$
SGRFT	$O\left[N_rN_{v3}N_{a3}N\right]$

The computational complexities of the four methods are compared in Fig. 2. The number of the range cells is supposed to be 500, i.e., $N_r = 500$. The searching number of the velocity of KT-TRT is supposed to be 1, i.e., $N_{v2} = 1$. The numbers of the velocity searching and the acceleration searching of SGRFT are supposed to be equal to N, i.e. $N_{v2} = N_{a2} = N$. The searching number of the velocity of the proposed method is $N_{v1} = N_{v2}/Q$ and it can be derived that $Q = 130$ according to Table 2. We and see that the proposed method reduces computational complexity significantly compared with SGRFT and the proposed method has similar computational complexity with SDFC-LVT.

V. NUMERICAL EXPERIMENTS

A. COHERENT INTEGRATION FOR MULTIPLE TARGETS

To prove the validity of the proposed method for multiple targets' coherent integration, two maneuvering targets are considered in the simulated experiment.

The motion parameters of the targets are listed in Table 3. The input SNRs of the Target 1 and the Target 2 are set as -3 dB and -6 dB, respectively. As we know, the long-time coherent integration is an effective way to improve the detection performance in the long range search radar and the radar in L-band is usually applied as the long range search radar. Therefore, the simulation parameters of the radar system are set as shown in Table 2

The simulation results of the proposed method are illustrated in Fig. 3. Fig. 3a shows the result after pulse com-

TABLE 2. Simulation parameters of the radar system.

Parameters	Values
Carrier frequency	1.3 GHz
Bandwidth	10 MHz
Sample frequency	25 MHz
PRF	2000 Hz
Pulse duration	10 us
Pulse number	1500

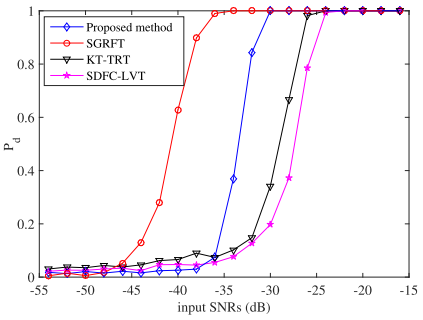

FIGURE 4. Detection probability of the four methods.

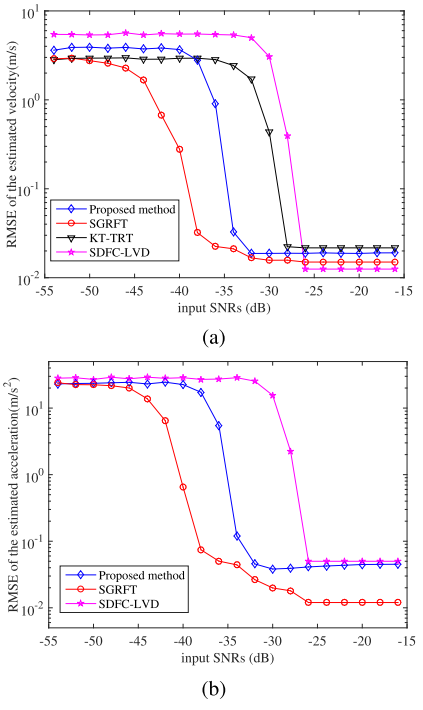

FIGURE 5. RMSE of the estimated motion parameters. (a) Velocity; (b) Acceleration.

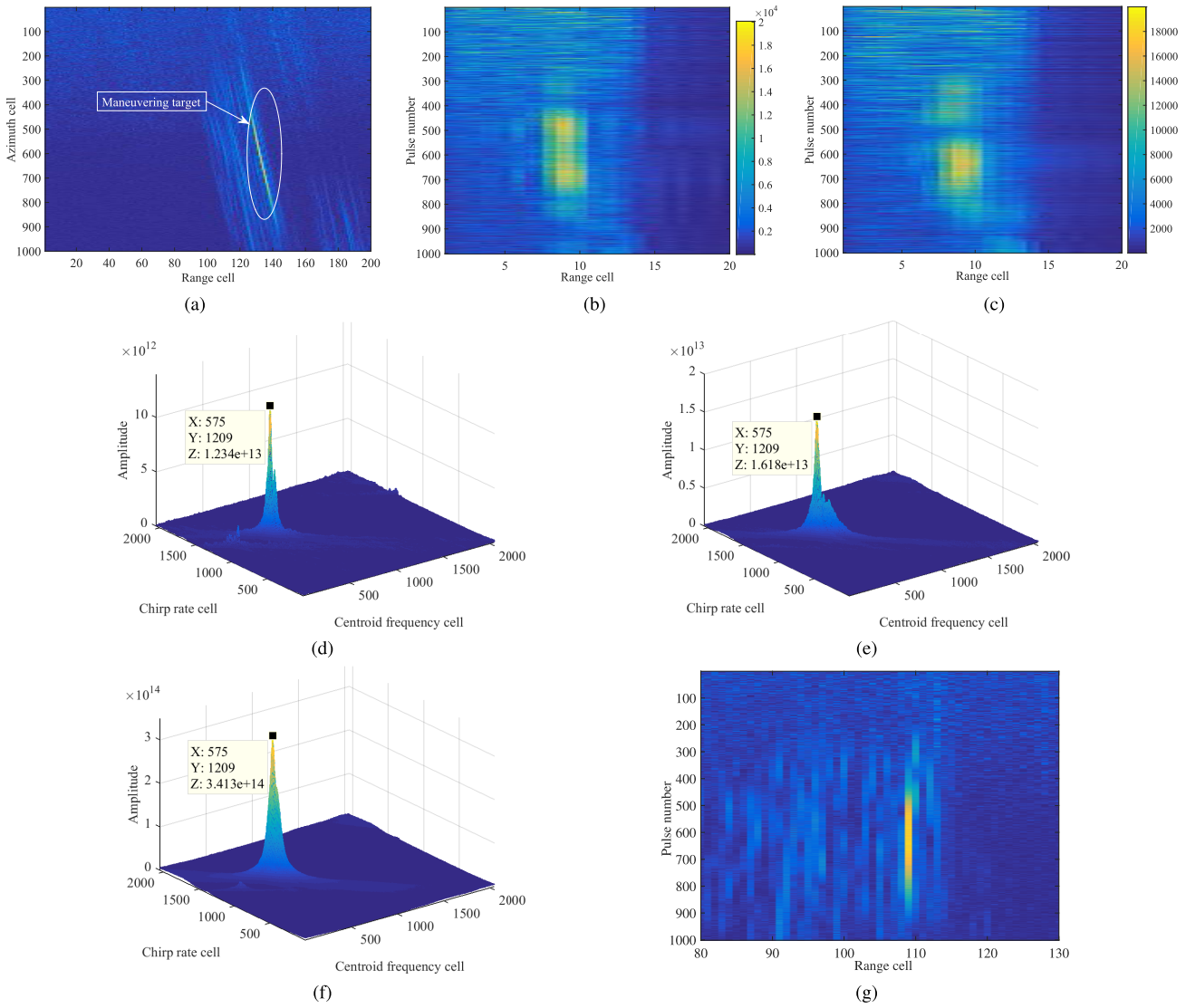

FIGURE 6. Results of the real data via the proposed method. (a) Trajectory of the received data after pulse compression; (b) Result of the first subband signal after FSSP; (c) Result of the last subband signal after FSSP; (d) LVD result of the first subband signal; (e) LVD result of the last subband signal; (f) The integrated LVD result of the all subband signals; (g) Result of the received data after RM correction with the estimated motion parameters.

TABLE 3. The motion parameters of the two targets.

Targets	Initial range	Radical velocity	Radical acceleration
Target 1	50 km	105 m/s	45 m/s^2
Target 2	50.03 km	100 m/s	50 m/s^2

pression. It can be observed from Fig. 3b that the total RM offsets of the targets are both 12 within the coherent integration time, which will cause the energy of the targets defocused. According to the RM offsets of both targets, the received signal is divided into 16 segments, that is $M = 16$. Fig. 3c and Fig. 3d show the results of the first and the last subband signals after FSSP, respectively, which indicate that the RM of both targets has been corrected effectively and the targets' energy has been in the same range cell. Fig. 3e and Fig. 3f show the LVD results of the first and the last subband signals after the phase compensation, respectively, which indicate that the peaks of different subband signals corresponding to the same target are in the same cell in the CFCR domain. Fig. 3g shows the integrated LVD result of all the subband signals. We can see that the targets' energy is coherently integrated as two peaks after the summation operation among all the subband signals. According to the peaks, the estimated motion parameters of Target 1 and Target 2 can be obtained, as shown in Table 4.

TABLE 4. The estimated values of the motion parameters.

Targets	Initial range	Radical velocity	Radical acceleration
Target 1	49.94 km	104.96 m/s	44.90 m/s^2
Target 2	49.94 km	99.91 m/s	50.04 m/s^2

B. PERFORMANCE ANALYSIS

The detection and estimation performance of SGRFT, SDFC-LVT, KT-TRT and the proposed method are further investigated by Monte Carlo trials. The constant false alarm ratio (CFAR) is set as $P_{fa} = 10^{-6}$. The input SNR varies from -54 dB to -16 dB with step size 2 dB. For each SNR, 1000 Monte Carlo simulations are performed.

Fig. 4 and Fig. 5 shows the detection probability and the RMSEs of the estimatedparameters of the four methods versus different input SNRs, respectively. We can see that the detection and estimation performance of the proposed method is superior to KT-TRT and SDFC-LVT in low SNR scenarios. Compared with SGRFT, the proposed method suffers some detection and estimation performance loss, which reduces computational complexity efficiently. The proposed method can achieve better detection performance in low SNR scenarios with closed computational complexity than SDFC-LVT. Compared with KT-SRT, the proposed method can achieve better detection performance in low SNR scenarios, though the proposed method needs larger computational complexity. Therefore, the proposed method can obtain a good balance between the computational cost and the detection and estimation performance.

C. REAL DATA RESULT ANALYSIS

Part of the RADARSAT-1 data (Vancouver scene) [30], [31] was used to further verify the effectiveness of the proposed method. The system parameters of the selected radar are given in Table 5 and the proposed method is performed to estimate the motion parameters of the selected target (labeled in Fig. 6a).

TABLE 5. Radar system parameters for real data.

System parameters	Values
Carrier frequency	5.3 GHz
Bandwidth	30.116 MHz
Sample frequency	32.317 MHz
PRF	1257 Hz
Pulse width	41.74 us

The experiment results of the proposed method using the real data are illustrated in Fig. 6. Fig. 6a shows the trajectory of the target after pulse compression, which indicates that serious RM occurs. According to the offset of the RM, the total number of the subband signals is set as 32. Fig. 6b and Fig. 6c show the results of the first and the last subband signals after FSSP, respectively, which indicates that the selected target's envelopes of each echoes are in the same range cell after FSSP. Fig. 6d and Fig. 6e show the LVD results of the first and the last subband signals after the phase compensation, respectively. Fig. 6f shows the integrated LVD result of the all subband signals. According to the location of the peak, the estimated velocity and acceleration are 206.62 m/s and -50.34 m/s^2, respectively, which are consistent with the estimated results in [22], [31]. Moreover, Fig. 6g shows the trajectory of the received signal after RM correction with the estimated parameters. It can be seen from Fig. 6g that the RM of the selected target is removed completely. Therefore, we can conclude that the estimated motion parameters are valid.

VI. CONCLUSION

This paper addresses range and Doppler frequency migrations caused by manoeuvring targets by applying segmenting the frequency spectrum for RM compensation and the Lv's distribution for DFM compensation. This work is based on the use of Linear Frequency Modulated signals and a detailed derivation of the migration correction is given. The estimation and detection performance against computational cost shows that the proposed method: (a) it can realize the coherent integration for multiple maneuvering targets without any prior knowledge of the targets' motion; (b) it offers a trade-off between computational load and detection probability compared to the state of the art in this area; (c) it is easy to implement to correct RM by fast Fourier transform and inverse fast Fourier transform. Moreover, the experimental results are persented to futher verify the effectiveness of the proposed method. As we know, the radar echoes are affected by clutter in strong clutter environment. In order to applying the work in real radar signal processing, some preprocessing steps should be performed on the echoes to suppress the clutter before coherent integration, such as space-time adaptive processing (STAP). We will focus our attention on this problem in the next work.

REFERENCES

[1] S. Zhu, G. Liao, D. Yang, and H. Tao, "A new method for radar high-speed maneuvering weak target detection and imaging," *IEEE Geosci. Remote Sens. Lett.*, vol. 11, no. 7, pp. 1175–1179, Jul. 2014.

[2] J. Zheng, J. Zhang, S. Xu, H. Liu, and Q. H. Liu, "Radar detection and motion parameters estimation of maneuvering target based on the extended keystone transform (July 2018)," *IEEE Access*, vol. 6, pp. 76060–76074, 2018.

[3] X. Li, G. Cui, W. Yi, and L. Kong, "A fast maneuvering target motion parameters estimation algorithm based on ACCF," *IEEE Signal Process. Lett.*, vol. 22, no. 3, pp. 270–274, Mar. 2015.

[4] J. D. Park and J. F. Doherty, "Track detection of low observable targets using a motion model," *IEEE Access*, vol. 3, pp. 1408–1415, 2015.

[5] P. Huang, G. Liao, Z. Yang, X.-G. Xia, J.-T. Ma, and J. Ma, "Long-time coherent integration for weak maneuvering target detection and high-order motion parameter estimation based on keystone transform," *IEEE Trans. Signal Process.*, vol. 64, no. 15, pp. 4013–4026, Aug. 2016.

[6] J. Xu, J. Yu, Y.-N. Peng, and X.-G. Xia, "Radon-Fourier transform for radar target detection, I: Generalized Doppler filter bank," *IEEE Trans. Aerosp. Electron. Syst.*, vol. 47, no. 2, pp. 1186–1202, Apr. 2011.

[7] J. Xu, X.-G. Xia, S.-B. Peng, J. Yu, Y.-N. Peng, and L.-C. Qian, "Radar maneuvering target motion estimation based on generalized radon-Fourier transform," *IEEE Trans. Signal Process.*, vol. 60, no. 12, pp. 6190–6201, Dec. 2012.

[8] R. P. Perry, R. C. Dipietro, and R. L. Fante, "SAR imaging of moving targets," *IEEE Trans. Aerosp. Electron. Syst.*, vol. 35, no. 1, pp. 188–200, Jan. 1999.

[9] S.-S. Zhang, T. Zeng, T. Long, and H.-P. Yuan, "Dim target detection based on keystone transform," in *Proc. IEEE Int. Radar Conf.*, May 2005, pp. 889–894.

[10] L. Kong, X. Li, G. Cui, W. Yi, and Y. Yang, "Coherent integration algorithm for a maneuvering target with high-order range migration," *IEEE Trans. Signal Process.*, vol. 63, no. 17, pp. 4474–4486, Sep. 2015.

[11] W. Cui, J. Xiang, and J. Tian, "Joint parameter estimation method for multiple manoeuvring targets with high speed," *IET Radar, Sonar Navigat.*, vol. 12, no. 5, pp. 530–539, May 2018.
[12] D. Kirkland, "Imaging moving targets using the second-order keystone transform," *IET Radar, Sonar Navigat.*, vol. 5, no. 8, pp. 902–910, Oct. 2011.
[13] J. Tian, W. Cui, and S. Wu, "A novel method for parameter estimation of space moving targets," *IEEE Geosci. Remote Sens. Lett.*, vol. 11, no. 2, pp. 389–393, Feb. 2014.
[14] S. Zhu, G. Liao, Y. Qu, Z. Zhou, and X. Liu, "Ground moving targets imaging algorithm for synthetic aperture radar," *IEEE Trans. Geosci. Remote Sens.*, vol. 49, no. 1, pp. 462–477, Jan. 2011.
[15] P. Huang, G. Liao, Z. Yang, X.-G. Xia, J. Ma, and X. Zhang, "An approach for refocusing of ground moving target without target motion parameter estimation," *IEEE Trans. Geosci. Remote Sens.*, vol. 55, no. 1, pp. 336–350, Jan. 2017.
[16] S. Peleg and B. Porat, "Estimation and classification of polynomial-phase signals," *IEEE Trans. Inf. Theory*, vol. 37, no. 2, pp. 422–430, Mar. 1991.
[17] E. J. Kelly, "The radar measurement of range, velocity and acceleration," *IRE Trans. Mil. Electron.*, vol. 5, no. 2, pp. 51–57, Apr. 1961.
[18] X.-G. Xia, "Discrete chirp-Fourier transform and its application to chirp rate estimation," *IEEE Trans. Signal Process.*, vol. 48, no. 11, pp. 3122–3133, Nov. 2000.
[19] L. B. Almeida, "The fractional Fourier transform and time-frequency representations," *IEEE Trans. Signal Process.*, vol. 42, no. 11, pp. 3084–3091, Nov. 1994.
[20] X. Lv, G. Bi, C. Wan, and M. Xing, "Lv's distribution: Principle, implementation, properties, and performance," *IEEE Trans. Signal Process.*, vol. 59, no. 8, pp. 3576–3591, Aug. 2011.
[21] S. Luo, G. Bi, X. Lv, and F. Hu, "Performance analysis on Lv distribution and its applications," *Digit. Signal Process.*, vol. 23, no. 3, pp. 797–807, May 2013.
[22] J. Tian, W. Cui, X. G. Xia, and S. L. Wu, "A new motion parameter estimation algorithm based on SDFC-LVT," *IEEE Trans. Aerosp. Electron. Syst.*, vol. 52, no. 5, pp. 2331–2345, May 2016.
[23] X. Li, G. Cui, W. Yi, and L. Kong, "Coherent integration for maneuvering target detection based on radon-Lv's distribution," *IEEE Signal Process. Lett.*, vol. 22, no. 9, pp. 1467–1471, Sep. 2015.
[24] X. Chen, J. Guan, N. Liu, and Y. He, "Maneuvering target detection via radon-fractional Fourier transform-based long-time coherent integration," *IEEE Trans. Signal Process.*, vol. 62, no. 4, pp. 939–953, Feb. 2014.
[25] X. Chen, J. Guan, Y. Huang, N. Liu, and Y. He, "Radon-linear canonical ambiguity function-based detection and estimation method for marine target with micromotion," *IEEE Trans. Geosci. Remote Sens.*, vol. 53, no. 4, pp. 2225–2240, Apr. 2015.
[26] E. L. Key, E. N. Fowle, and R. D. Haggarty, "A method of designing signals of large time-bandwidth product," *IRE Int. Conv. Rec.*, vol. 4, pp. 146–154, Mar. 1961.
[27] P. Swerling, "Probability of detection for fluctuating targets," *IEEE Trans. Inf. Theory*, vol. 6, no. 2, pp. 269–308, Apr. 1960.
[28] M. I. Skolnik, *Introduction To Radar System*, 3rd ed. New York, NY, USA: McGraw-Hill, 2002.
[29] P. Wang, H. Li, I. Djurovic, and B. Himed, "Integrated cubic phase function for linear FM signal analysis," *IEEE Trans. Aerosp. Electron. Syst.*, vol. 46, no. 3, pp. 963–977, Jul. 2010.
[30] I. G. Cumming and F. H. Wong, *Digital Processing of Synthetic Aperture Radar Data Algorithms and Implementation*. Norwood, MA, USA: Artech House, 2005.
[31] J. Tian, W. Cui, X.-G. Xia, and S.-L. Wu, "Parameter estimation of ground moving targets based on SKT-DLVT processing," *IEEE Trans. Comput. Imag.*, vol. 2, no. 1, pp. 13–26, Mar. 2016.

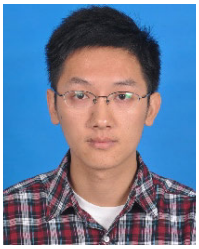

JINZHI XIANG was born in Hunan, China, in 1990. He received the B.S. and Ph.D. degrees in electronic engineering from the Beijing University of Posts and Telecommunications and the Beijing Institute of Technology, in 2012 and 2018, respectively. He is currently an Engineer with the Second Academy of China Aerospace, Beijing. His research interests include moving target detection and array signal processing.

WEI CUI (Member, IEEE) was born in Inner Mongolia, China, in 1976. He received the B.S. degree in physics and the Ph.D. degree in electronics engineering from the Beijing Institute of Technology, Beijing, China, in 1998 and 2003, respectively. From March 2003 to March 2005, he held a postdoctoral position at the School of Electronic and Information Engineering, Beijing Jiaotong University. Since then, he has been with the Beijing Institute of Technology, where he is currently a Professor with the School of Information and Electronics. His research interests include adaptive signal processing, array signal processing, sparse signal processing, and their various applications such as radar and aerospace TT&. He has published more than 100 articles, held 17 patents, and received the Ministerial Level Technology Advancement Award thrice.

JING TIAN (Member, IEEE) was born in Shandong, China, in November 1984. She received the B.S. and Ph.D. degrees in electrical engineering from Xidian University and the Beijing Institute of Technology, in 2006 and 2014, respectively. She worked as a Postdoctoral Researcher at the Second Academy of China Aerospace, Beijing. She currently works as an Associate Professor at the Beijing Institute of Technology. Her research interests include moving-target detection, parameter estimation, and imaging.